Accepted Manuscript

Texture evolution during annealing of hot extruded U-10wt%Zr alloy by in situ neutron diffraction

S. Irukuvarghula, B. Blamer, S. Ahn, S.C. Vogel, A. Losko, S.M. McDeavitt

PII: S0022-3115(17)30468-3

DOI: 10.1016/j.jnucmat.2017.09.008

Reference: NUMA 50494

To appear in: *Journal of Nuclear Materials*

Received Date: 22 March 2017

Revised Date: 31 July 2017

Accepted Date: 6 September 2017

Please cite this article as: S. Irukuvarghula, B. Blamer, S. Ahn, S.C. Vogel, A. Losko, S.M. McDeavitt, Texture evolution during annealing of hot extruded U-10wt%Zr alloy by in situ neutron diffraction, *Journal of Nuclear Materials* (2017), doi: 10.1016/j.jnucmat.2017.09.008.

Texture evolution during annealing of hot extruded U-10wt%Zr alloy by in situ neutron diffraction

S. Irukuvarghula *[1], B. Blamer[1], S. Ahn[2], S. C. Vogel[3], A. Losko[3], and S. M. McDeavitt[1]

[1]Department of Nuclear Engieering, Texas A&M University, College Station, TX, 77843, U.S.A

[2]Department of Nuclear Engieering, UNIST, South Korea

[3]Materials Science and Technology Division, Los Alamos National Laboratory, NM, U.S.A

Abstract

Texture evolution during annealing of a U-10wt%Zr alloy hot extruded in the $(\alpha+\delta)$ region was studied by in situ neutron diffraction. The extruded alloy had a lamellar $(\alpha+\delta)$ microstructure and the initial texture consisted of $(100)_\alpha$, $(110)_\alpha$, and the $(0001)_\delta$ poles oriented along the extrusion direction. The β phase, after the $\alpha \rightarrow \beta$ transformation, showed no preferred orientation while the γ phase, after the $\beta \rightarrow \gamma$ transformation, had $(110)_\gamma$ and $(111)_\gamma$ poles oriented along the extrusion direction. After a temperature cycle through the γ phase, there was a complete loss of texture in the α phase while the δ phase retained the initial texture indicating a memory effect.

Keywords: **Uranium, Zirconium, Extrusion, Texture, Neutron diffraction**

1 Introduction

High thermal conductivity and the ability to incorporate minor actinides makes metallic fuels an attractive choice for fast reactors [1]. Additionally, irradiation data from one of the alloy compositions, i.e., uranium-10wt% zirconium (U-10Zr) alloys available from the

*Present address: School of Materials, University of Manchester. Corresponding author: sandeep.irukuvarghula@manchester.ac.uk

Experimental Breeder Reactor-II (EBR)[1] indicate their viability as a potential fuel form [2]. U-Zr alloy fuel rods can be produced by different processes like injection casting, machining, and extrusion. Injection casting requires very high temperatures and expensive crucibles while machining results in large material losses. Extrusion may be a favourable alternative to other methods since it is more cost effective. It is a common fabrication process that is performed on an industrial scale around the world to cost-effectively manufacture many simple shapes from many materials such as aluminum, copper, and steel [3]. Extrusion of uranium or its alloys is not a common practice; however, it has been previously investigated to some detail where extruded fuel pins were tested in EBR-I [1]. The present study is aimed towards the evaluation of extrusion as a potential manufacturing process for U-10Zr fuel pins by understanding the microstructural changes of a hot extruded billet during annealing.

Uranium and its alloys undergo several phase transformations with temperature: pure uranium occurs in the orthorhombic α-phase at room temperature, followed by a transition at 669 °C to the tetragonal β-phase, and at 776 °C to the body centered cubic (bcc) γ-phase [4]. In the U-Zr system studied here, α, β, γ along with δ are relevant within the context of this work. Here, the δ-phase is hexagonal and exists along with α at room temperature (U-Zr phase diagram is shown in Fig. 1). Because of the strong thermoelastic and plastic anisotropy exhibited by α-U, any thermo-mechanical processing in the α phase results in the texture development [5, 6, 7].

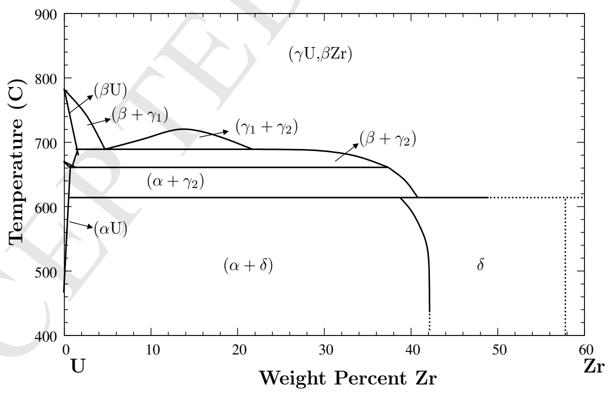

Figure 1: A sketch of the U-rich end of the U-Zr phase diagram showing phases relevant to this study [4].

Since the present study deals with hot extrusion of U-10Zr alloy in the $(\alpha+\delta)$ region, relevant literature on the textures developed in α-U during various thermomechanical processing conditions is briefly reviewed. It has been observed that the texture developed in α-U not only depends on the nature of the deformation (compression, tension, rolling, extrusion), but also on the temperature at which the specimen is deformed [8, 9, 10,

[1]The U-10Zr alloy had $(\alpha+\delta)$ as starting microstructure [2].

11, 12, 13, 14]. This is due to the strong dependence of the relative importance of the deformation modes on temperature (i.e., slip and twinning) in uranium [7, 12, 15]. Daniel et al [7], by deforming the specimens under tension and compression, have shown that at all temperatures, slip occurs most easily in the [100] direction, and depending on the temperature, it would occur on the (010) plane below 500 °C, or on (001) plane at higher temperatures. Slip on the (110) plane and [110] direction was observed at temperatures above 150 °C. Ivanov et al [12] have observed that at rolling temperatures above 300 °C, twinning becomes less pronounced while the dominant slip system is $\{110\}\langle 110\rangle$. It has been pointed out that, with increasing temperature, the critical stress for activating slip decreases much more rapidly than for twinning [15].

Previously observed deformation textures in α-U correspond, in the case of warm rolling, to (010) poles aligning with the rolling direction and (001) poles aligning along the normal direction to rolling [9, 14, 16], and in extruded uranium and U-2.4 wt%Nb alloy, to (110) poles aligning in the extrusion direction in samples subjected to low extrusion ratio and near the (310)-(100) region in samples subjected to a high extrusion ratio, respectively [11, 13]. Complete loss of α texture was observed after the $\alpha \rightarrow \beta \rightarrow \gamma \rightarrow \beta \rightarrow \alpha$ transformation cycle while a texture memory effect was observed after the $\alpha \rightarrow \beta \rightarrow \alpha$ transformation cycle, the reason for which was attributed to the retention of small nuclei of the parent α in the β phase ([17] and references there in). Deformation textures of the intermetallic UZr_2-δ phase in U-Zr alloys, which is hexagonal, have not been published in the literature and the texture development for the specific case where thermo-mechanical processing is performed in the $(\alpha + \delta)$ region, is not yet reported.

In regards to metallic uranium or any uranium based metallic alloy fuels, it was observed that the α-U phase undergoes anisotropic irradiation growth [18]. Specifically, due to the anisotropic properties of the orthorhombic crystal structure of α-U, mismatched strains develop between individual grains due to their anisotropic growth during irradiation. The stresses thus developed accumulate and can be released at grain boundaries causing "tearing or cavitation swelling" [2]. Since cavitational swelling is the consequence of anisotropic irradiation growth in α-U, preferred orientation of α-U grains resulting from the manufacturing process plays very important role in influencing the shape changes of fuel pin during irradiation. In U-Zr alloy fuel pins, cavitational swelling was observed in the region where the fuel pin had $(\alpha + \delta)$ microstructure [2]. However, the irradiation response of monolithic δ phase is not yet known. In order to preserve the dimensional stability of the fuel pins during service, the fuel material must be texture free, which imposes challenges on the manufacturing process. Due to the complex interplay of phase transformations, alloying element redistribution, recrystallization etc during heat treatments, experimental in situ data is of great value to understand and ultimately predict and optimize the microstructure during manufacturing [2]. In the present paper, we report the results from our study on the texture evolution during annealing of a U-10Zr alloy extruded at 600 °C, in the $(\alpha + \delta)$ region in situ, using neutron diffraction. The results will be used to optimize the extrusion process parameters and subsequent heat treatments to obtain a microstructure, which is texture and residual stress free.

2 Experimental

Depleted uranium (DU) pieces were pickled in 25 vol% nitric acid to remove the oxide layer before casting. DU pieces and crystal bar zirconium were then weighed such that the alloy contained 10 wt% Zr, and melt cast in yttrium oxide crucibles under argon atmosphere in a high temperature furnace with a heating rate of 20 °C/min. The alloy was held isothermally for 2 hours at 1900 °C (U-10Zr composition melts at around 1400 °C) after which it was cooled (i.e., furnace cooled under argon atmosphere) at a rate of about 20 °C/min to ambient temperature. To ensure homogeneity of the alloy, the ingot was re-melted affer flipping, using the same temperature cycle. The as-cast ingot had a diameter of 19 mm. It was then extruded at 600 °C using a rig that was housed in a custom built enclosure that has flowing argon, using a force of 306 kN. The area reduction was about 11.1 and the extrusion constant K was 65. Post-extrusion cooling to room temperature was under flowing argon. Oxygen content after casting and extrusion was not measured in the sample. Rough et al. have shown that oxygen and nitrogen impurities can make α-U and α-Zr more stable than the δ phase [19]. In addition, a general feature that is reported in the literature is the presence of impurity (oxygen and carbon) stabilized Zr precipitates [20]. As will be shown in the subsequent section, impurity stabilized α-Zr precipitates were found in the extruded alloy..

Texture measurement using neutron diffraction was performed on the time-of-flight diffractometer HIPPO at the pulsed neutron source at LANSCE [21]. A resistive furnace with vanadium heating elements was used to collect the diffraction patterns under vacuum at high temperatures [22]. The large angular detector coverage and very high neutron count rates for the instrument have been effectively used in order to optimise the data collection time. Data were first acquired for 4 sample rotations (0 °, 22.5 °, 45 °, and 135 ° about vertical axis) and then for 3 rotations (45 °, -22.5 °, and -45 °), with 3 minutes exposure time for each rotation using the 150 °, 120 °, 90 °, 60 °, and 40 ° detector banks. The sample rotations along the vertical axis improve the detector coverage; specific details about the instrument and data collection procedure can be found in [21, 22, 23]. Data analysis was performed following procedures outlined in [23] using the E-WIMV method to determine the orientation distribution function. Individual pole figures were recalculated using MTEX software after exporting the data from MAUD (Materials Analysis Using Diffraction) [24]. Analysis indicated that both data sets gave similar results for the texture; subsequently, 3 rotations were used for collecting the diffraction patterns. Diffraction patterns at non-ambient temperatures (at 200 °C during heating and at 600 °C, 650 °C, 680 °C, 700 °C, and 800 °C during heating and cooling) were collected to monitor the texture evolution as the phase transformations occur. The temperatures were selected based on the phase diagram [4] and from the differential scanning calorimetry (DSC) measurements on the as-cast alloy [25], shown in Table. 1. Texture data for the room temperature equilibrium phases, i.e., α and δ are first presented followed by the data for high temperature phases, i.e., for β (after $\alpha \rightarrow \beta$ transformation) and γ (after $\delta \rightarrow \gamma$ and $\alpha \rightarrow \beta \rightarrow \gamma$ transformations).

Table 1: Phase transformations and the associated temperatures (in °C) in U-10Zr alloy

Phase transformations†	$(\alpha+\delta) \rightarrow (\alpha+\gamma)$	$(\alpha+\gamma) \rightarrow (\beta+\gamma)$	$(\beta+\gamma) \rightarrow \gamma$
Phase diagram	617	662	693
DSC measurement	617.5	680‡	695

† α: Orthorhombic; β: Tetragonal; γ: Body centered cubic; δ (intermetallic with UZr_2 stoichiometry): Hexagonal.

‡ It is seen that the $(\alpha+\gamma) \rightarrow (\beta+\gamma)$ transformation occured at much higher temperature than what is shown in the phase diagram. This aspect is addressed elsewhere [26].

3 Results

Fig. 2a shows the microstructure of extruded alloy, which has a lamellar microstructure consisting of α and δ-UZr_2 phases. The high density of dark contrast features correspond to the δ-UZr_2 phase while the highest contrast features, which are elongated in the extrusion direction (indicated by an arrow in Fig. 2a), correspond to zirconium stringers. Volume fractions of the phases were not estimated from the image. The neutron diffraction pattern collected at the 150 ° detector bank for 22.5 ° sample rotation is shown in Fig. 2b confirmed the presence of α and δ phases. Rietveld refinement resulted in the weight fractions of around 0.80 and 0.20 for α and δ phase, respectively, in good agreement with the U-Zr phase diagram (0.78 and 0.22 for α and δ, respectively) [4].

The (100), (010), (001), and (110) pole figures for α in the as-cast alloy are shown in Fig. 3a; it is seen that the texture is quite random. For the extruded alloy, the room temperature α pole figures reveal that the $(100)_\alpha$ and $(110)_\alpha$ poles are oriented along the extrusion direction (Fig. 3b). At 600 °C, within the $(\alpha+\delta)$ region, no significant change in texture is observed (Fig. 3c) while at 650 °C, in the $(\alpha+\gamma)$ region, the α texture weakens (Fig. 3d). However, after heating to 800 °C and cooling the sample back, i.e., after the $\alpha \rightarrow \beta \rightarrow \gamma \rightarrow \beta \rightarrow \alpha$ transformation cycle, the α texture is completely lost (Fig. 3e), in accord with the observations in [13, 17].

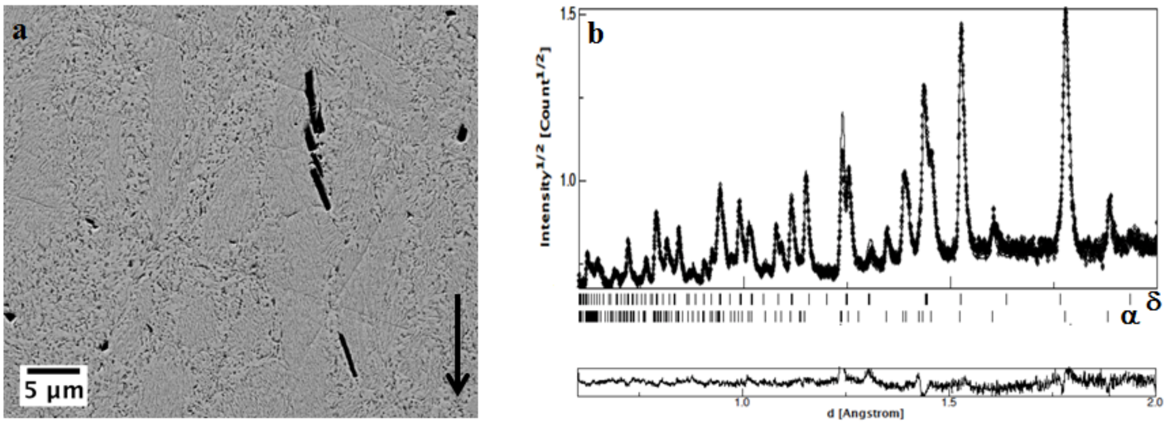

Figure 2: (a) Back scattered electron image of the extruded alloy showing two phase ($\alpha + \delta$) microstructure. The extrusion direction is indicated by an arrow. (b) Neutron diffraction pattern of the extruded alloy along with the Rietveld fit from the 150 ° detector bank at 22.5 ° sample rotation, taken at room temperature.

The pole figures for δ phase in the as-cast alloy are shown in Fig. 4a; it is seen that it has very weak texture, developed during casting where $(0001)_\delta$ poles are aligned parallel to the rod axis. For the extruded alloy, at room temperature, the $(0001)_\delta$ poles are oriented along the extrusion direction (Fig. 4b). This texture is preserved at 200 °C and 600 °C during heating. The orientation distribution with c-axes aligned along the extrusion direction starts to break up into distinct maxima with a larger spread around the extrusion direction with c-axis maxima even observed approximately radially at 600 °C (Fig. 4c and Fig. 4d, respectively).

After heating the sample to 800 °C and cooling back, i.e., after the $\delta \rightarrow \gamma \rightarrow \delta$ transformation cycle, the texture was analysed at 600 °C and the pole figures are shown in Fig. 4e. It is seen that the $(0001)_\delta$ texture is preserved indicating a memory effect. Comparing the pole figures at room temperature and after the thermal cycle (Fig. 4b and 4e), spottiness is observed, suggesting the presence of few large grains.

The pole figures for β phase at 680 °C, after the $\alpha \rightarrow \beta$ transformation, show that it has a random texture (Fig. 5a). Even though no conclusive orientation relationship for the $\alpha \rightarrow \beta$ transformation is known [17], several possible variants are likely and the relatively weak α texture (max. of ∼2.5 multiples of random distribution) results in a random texture of the β phase.

The γ phase texture is shown at 650 °C in the ($\alpha + \gamma$) phase field after the partial $\delta \rightarrow \gamma$ transformation, 700 °C, after the partial $\beta \rightarrow \gamma$ transformation at which point the alloy is completely in the γ phase, 800 °C during heating, and at 700 °C during cooling in Fig. 5b, 5c, 5d, and 5e, respectively. It is pointed out that though the diffraction peaks for γ phase completely overlap with those of α, the texture of γ, though weak, is

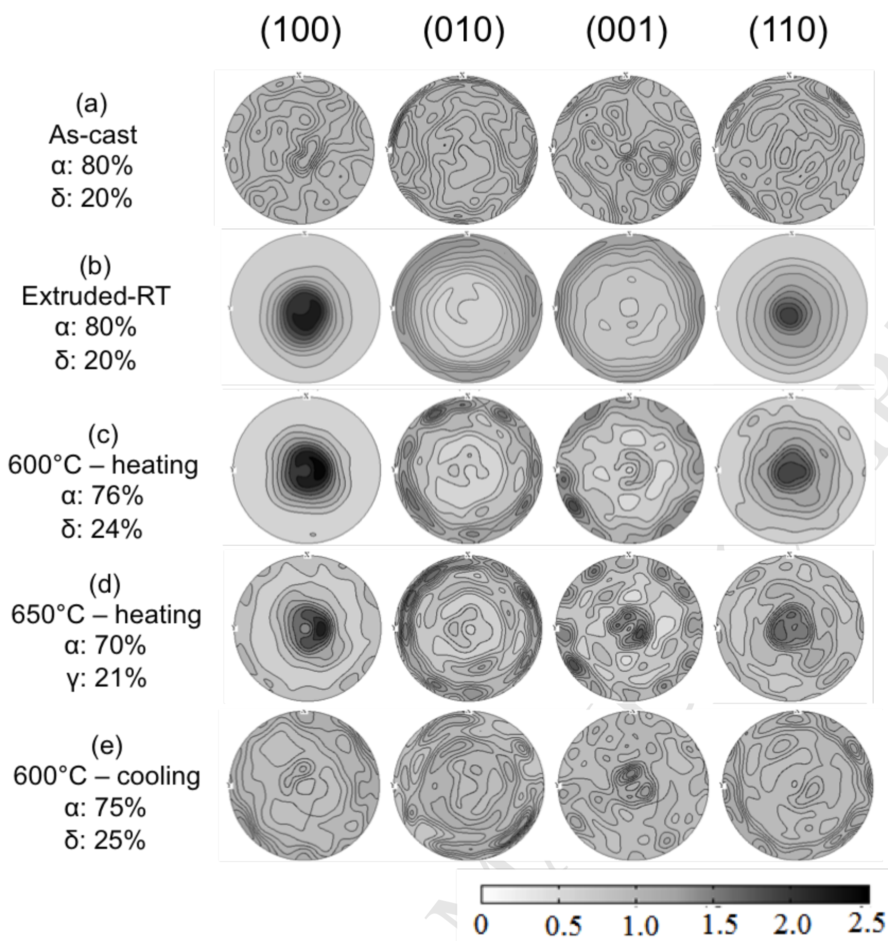

Figure 3: Pole figures of α-U (a) of as-cast alloy (b) Extruded alloy at room temperature (RT) (c) at 600 °C during heating (d) at 650 °C during heating (e) at 600 °C during cooling. The phases along with their weight fractions present at each temperature from the Rietveld refinement are also shown. At 650 °C, 9% of β-U was found to be present. Extrusion direction is at the centre.

captured quite nicely at 650 °C (in the $(\alpha + \gamma)$ region). It is seen that $(110)_\gamma$ and $(111)_\gamma$ poles are aligned in the extrusion direction. This becomes quite clear when compared with the texture, which is stronger, obtained at 700 °C and 800 °C, where the sample has 100% γ phase (Fig. 5c, 5d, and 5e).

4 Discussion

In the present study, the preferred orientation developed in α-U after extrusion is in agreement with the ones reported in literature [11, 13]. While the complete loss of α texture after the $\alpha \rightarrow \beta \rightarrow \gamma \rightarrow \beta \rightarrow \alpha$ transformation cycle observed in this study in situ by capturing the texture changes in various phase fields is in accord with the published literature (note, in previous studies these were performed ex situ at room

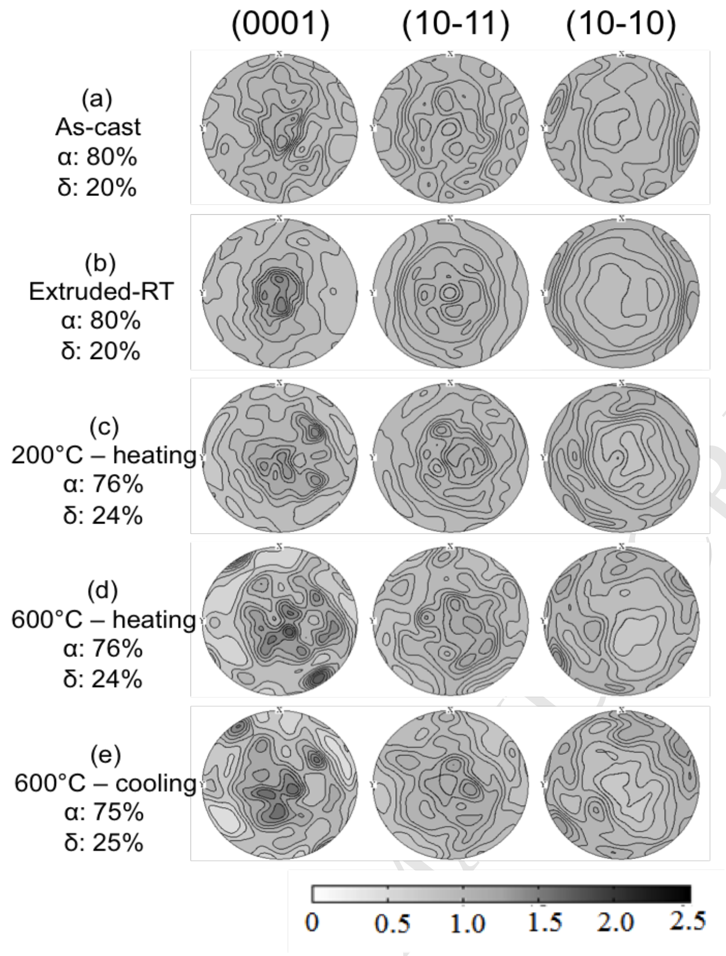

Figure 4: Pole figures of δ-UZr_2 (a) in the as-cast alloy (b) Extruded alloy at room temperature (RT) (c) at 200 °C (d) at 600 °C during heating (e) at 600 °C during cooling. The pole figures are plotted to the same scale as in α. The phases along with their weight fractions present at each temperature obtained from the Rietveld refinement are also shown. Extrusion direction is at the centre.

temperature, after the transformation cycle), perhaps the most interesting result is the texture memory effect observed for the δ phase.

Basak et al [27] have shown that δ phase forms from the high temperature γ phase via ω transformation mechanism and is related to γ by the following orientation relationship (OR): $(111)_\gamma \parallel (0001)_\delta$ and $\langle\bar{1}10\rangle_\gamma \parallel \langle11\bar{2}0\rangle_\delta$. Specifically, the δ phase forms by the collapse of alternate $(111)_\gamma$ planes in opposite direction with the third plane unaltered to form the intermediate $(0001)_\delta$ plane, followed by the partial ordering of U and Zr atoms in the hexagonal cell and has four possible variants.

DSC data for U-10Zr alloy published elsewhere have shown the following [25]: (a) from the cooling curve, the high temperature γ phase first transforms partially to α at 663 °C and the remnant γ then transforms to δ at 616 °C producing the $(\alpha + \delta)$ microstructure at room temperature and (b) from the heating curve, the $\delta \rightarrow \gamma$ transformation occurs

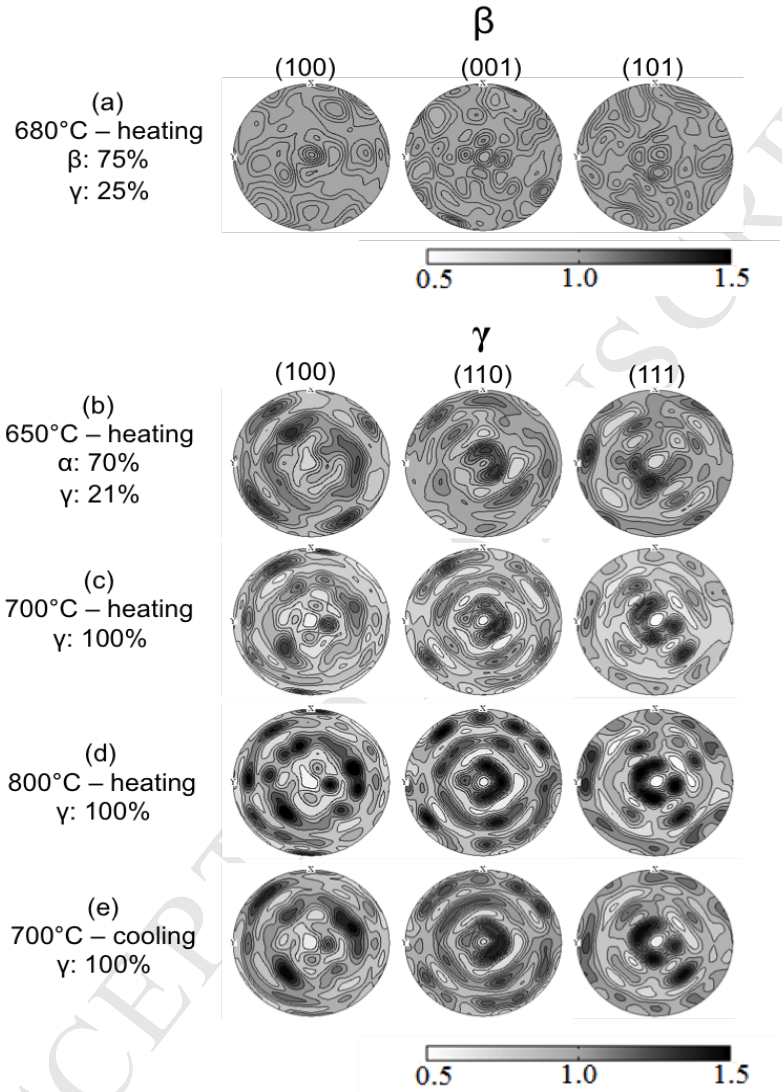

Figure 5: Pole figures of extruded alloy for (a) β-U at 680 °C (b) γ-U at 650 °C during heating (c) γ-U at 700 °C during heating (d) γ-U at 800 °C during heating (e) γ-U at 700 °C during cooling. The phases along with their weight fractions present at each temperature from the Rietveld refinement are also shown. At 650 °C, 9% of β-U was found to be present. Extrusion direction is at the centre.

at 617.5 °C. As described above, during cooling, the $\gamma \rightarrow \delta$ transformation at 616 °C happens by the collapse of $(111)_\gamma$ planes to form $(0001)_\delta$ planes.

The microstructural development observed in the present study can be rationalized in the following way. For U-10Zr alloy, while heating, the following transformations occur as per the equilibrium phase diagram: from the room temperature ($\alpha + \delta$) with ∼34 vol% δ and 66 vol% α, the δ phase first transforms to γ at 617 °C. The α transforms to β at 662 °C and at 693 °C, β transforms to γ. The alloy, when it is 100% γ (i.e., at 700 °C), will contain some fraction (i.e., 34 vol%) resulting from $\delta \rightarrow \gamma$ and the rest (i.e., 66 vol%) from $\alpha \rightarrow \beta \rightarrow \gamma$. So, when the alloy is extruded in the ($\alpha + \delta$) region, one would expect the texture developed for the δ phase and the one for the γ phase after $\delta \rightarrow \gamma$ transformation to be related by the OR: $(0001)_\delta \parallel (111)_\gamma$. Comparing the pole figures of $(0001)_\delta$ at 600 °C and $(111)_\gamma$ at 650 °C (Fig. 4d and 5b respectively), the OR is not clearly reflected.

When the alloy is 100% γ, the texture is much stronger than it is at 650 °C (Fig. 5b, c, d, and e) and can be interpreted in the following way: the high temperature γ (i.e., at temperatures >700 °C where it is 100% γ) forms, as mentioned above, from two different transformation paths; some as a result of $\delta \rightarrow \gamma$ and the rest via $\alpha \rightarrow \beta \rightarrow \gamma$ transformation. So, the texture of γ should reflect the OR with δ and an OR with β (i.e., after $\alpha \rightarrow \beta \rightarrow \gamma$). However, β texture is quite random (Fig. 5a) and an OR between β and γ has not been established yet, mainly because of the difficulty in retaining both phases simultaneously. From Fig. 5c, d, and e, it is seen that $(110)_\gamma$ and $(111)_\gamma$ poles are aligned along the extrusion direction. While the $(111)_\gamma$ texture suggests the presence of an OR with δ (i.e., $(111)_\gamma \parallel (0001)_\delta$), the matching is not sufficient to claim its presence. The $(110)_\gamma$ texture does not seem to be related to either β or α.

The texture memory of δ phase after the temperature cycle suggests that only those γ grains that have formed as a result of $\delta \rightarrow \gamma$ during heating have again transformed to δ during cooling. Because of the relatively moderate starting texture of δ phase, and the added complexity of phase transformations involving α and β at high temperatures (i.e., $\alpha \rightarrow \beta \rightarrow \gamma$), the OR between δ and γ was not clearly reflected in the pole figures. A similar experiment on a deformed U-50Zr alloy, which contains 100% δ from room temperature to around 600 °C, would help clarify the texture memory effect as this alloy composition only undergoes $\delta \rightarrow \gamma$ transformation. Since the preferred orientation of α phase is lost after a phase transformation cycle (i.e., upon $\alpha \rightarrow \beta \rightarrow \gamma \rightarrow \beta \rightarrow \alpha$), studies on the possibility of randomizing the δ texture by suitable heat treatments and on the irradiation response of δ phase for possible anisotropic swelling effects need to be carried out.

Conclusions

In summary, we have carried out an in situ neutron diffraction study to monitor the texture evolution during annealing in a U-10Zr alloy hot extruded in $(\alpha + \delta)$ region. The results show a complete loss of α texture and suggest a texture memory effect for the δ phase after the $\alpha \rightarrow \beta \rightarrow \gamma \rightarrow \beta \rightarrow \alpha$ and $\delta \rightarrow \gamma \rightarrow \delta$ transformation cycles, respectively.

Acknowledgements

This work has benefited from the use of HIPPO diffractometer at the Lujan Center at Los Alamos Neutron Science Center. Los Alamos National Laboratory is operated by Los Alamos National Security LLC under DOE Contract DE-AC52-06NA25396.

References

[1] D. E. Burkes, R. S. Fielding, D. L. Porter, D. C. Crawford, and M. K. Meyer. A US perspective on fast reactor fuel fabrication technology and experience part I: metal fuels and assembly design. *J. Nucl. Mater.*, 389(3):458–469, 2009.

[2] G. L. Hofman, L. C. Walters, and T. H. Bauer. Metallic fast reactor fuels. *Prog. Nucl. Ener.*, 31(1):83–110, 1997.

[3] M. Bauser and K. Siegert. *Extrusion: Second Edition*. ASM International, 2006.

[4] R. I. Sheldon and D. E. Peterson. The U-Zr (Uranium-Zirconium) System. *Bull. Alloy Phase Diag.*, 10:165–171, 1989.

[5] R. W. Cahn. Plastic deformation of alpha-uranium; twinning and slip. *Acta Metall.*, 1(1):49 – 70, 1953.

[6] A. G. Crocker. The crystallography of deformation twinning in alpha-uranium. *J. Nucl. Mater.*, 16(3):306 – 326, 1965.

[7] J. S. Daniel, B. Lesage, and P. Lacombe. The influence of temperature on slip and twinning in uranium. *Acta Metall.*, 19(2):163 – 173, 1971.

[8] E. A. Calnan and C. J. B. Clews. The prediction of uranium deformation textures. *Philos. Mag.*, 43(336):93–104, 1952.

[9] G. B. Harris. Quantitative measurement of preferred orientation in rolled uranium bars. *Philos. Mag.*, 43(336):113–123, 1952.

[10] L. K Jetter and C. J McHargue. Preferred orientation in extruded uranium rod. *Trans. Am. Inst. Min. Metall. Pet. Eng.*, 209:291–292, 1957.

[11] J. Laniesse, P. Meriel, and M. Englander. Etude aux neutrons de la texture cristalline de barreaux d'uranium. *J. Nucl. Mater.*, 2(1):69 – 74, 1960.

[12] V. E. Ivanov, V. F. Zelenskii, V. V. Kunchenko, N. M. Roenko, V. S. Krasnorutskii, and V. P. Ashikhmin. Influence of impurity state on the deformation texture of slightly alloyed α-uranium. *Sov. Atom. Ener.*, 24(1):103–107, 1968.

[13] D. A. Carpenter, S. H. Rogers, Kollie T. G., and R. C. Anderson. *Phase and texture analysis of the alpha-phase extruded uranium-2.4 weight percent niobium alloy.* Dec 1981.

[14] D. W. Brown, M. A. M. Bourke, B. Clausen, D. R. Korzekwa, R. C. Korzekwa, R. J. McCabe, T. A. Sisneros, and D. F. Teter. Temperature and direction dependence of internal strain and texture evolution during deformation of uranium. *Mater. Sci. Eng. A*, 512(1–2):67 – 75, 2009.

[15] J. L. Francois. *The plastic deformation of polycrystalline uranium between 20 and 660 °C.* PhD thesis, University of Paris, 1968.

[16] C. A. Calhoun, E. Garlea, T. Sisneros, and S. R. Agnew. Effects of hydrogen on the mechanical response of α-uranium. *J. Nucl. Mater.*, 465:737 – 745, 2015.

[17] A. Goldberg and T. B. Massalski. *Phase Transformations in the Actinides.* Jan 1970.

[18] S. H. Paine and J. H. Kittel. *Proceedings of the First International Conference on the Peaceful Uses of Atomic Energy: Geneva, 8-20 August 1955*, volume 7. UN, 1955.

[19] F. A. Rough, A. E. Austin, A. A. Bauer, and J. R. Doig. The stability and existence range of the Zirconium-Uranium Epsilon phase. BMI-1092, Battelle Memorial Institute, 1956.

[20] G. L. Hofman, R. G. Pahl, C. E. Lahm, and D. L. Porter. Swelling Behavior of U-Pu-Zr Fuel. *Metallurgical Transactions A*, 21:517–528, 1990.

[21] H. R. Wenk, L. Lutterotti, and S. Vogel. Texture analysis with the new HIPPO TOF diffractometer. *Nucl. Instr. Meth. Phys. Res. A*, 515(3):575 – 588, 2003.

[22] S. C. Vogel, C. Hartig, L. Lutterotti, R. B. Von Dreele, H. R. Wenk, and D. J. Williams. Texture measurements using the new neutron diffractometer HIPPO and their analysis using the rietveld method. *Powder Diffraction*, 19:65–68, 3 2004.

[23] H. R. Wenk, L. Lutterotti, and S. C. Vogel. Rietveld texture analysis from TOF neutron diffraction data. *Powder Diffract.*, 25:283–296, 9 2010.

[24] R. Hielscher and H. Schaeben. A novel pole figure inversion method: specification of the *MTEX* algorithm. *J. Appl. Crystallogr.*, 41(6):1024–1037, Dec 2008.

[25] S. Irukuvarghula and S. M. McDeavitt. Formation Mechanism of Delta Phase in the As-cast U-10wt%Zr Alloy. *Trans. Amer. Nuc. Soc*, 109:612–615, 2013.

[26] S. Ahn, S. Irukuvarghula, and S. M. McDeavitt. Thermophysical investigations of the uranium–zirconium alloy system. *J. Alloy Compd.*, 611:355 – 362, 2014.

[27] C. B. Basak, S. Neogy, D. Srivastava, G. K. Dey, and S. Banerjee. Disordered bcc γ-Phase to δ-Phase Transformation in Zr-Rich U-Zr Alloy. *Philos. Mag.*, 91:3290–3306, 2011.